

Rapid Precipitation of Magnesite Microcrystals from $\text{Mg}(\text{OH})_2\text{-H}_2\text{O-CO}_2$ Slurry Enhanced by NaOH and a Heat-Aging Step (from ~ 20 to $90\text{ }^\circ\text{C}$)

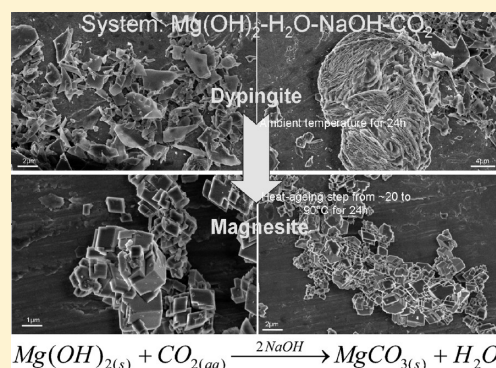
G. Montes-Hernandez,^{*,†} F. Renard,^{†,§} R. Chiriac,[‡] N. Findling,[†] and F. Toche[‡]

[†]ISTerre, CNRS and University of Grenoble I, BP 53, 38041 Grenoble Cedex 9, France

[‡]Université de Lyon, Université Lyon 1, Laboratoire des Multimatériaux et Interfaces UMR CNRS 5615, 43 bd du 11 novembre 1918, 69622 Villeurbanne Cedex, France

[§]Physics of Geological Processes, University of Oslo, Oslo, Norway

ABSTRACT: This study proposes a simple and novel synthesis route for rhombohedral single crystals ($<2\ \mu\text{m}$) of magnesite. This synthesis can be summarized by two main sequential reactions: (1) aqueous carbonation of synthetic brucite ($\text{Mg}(\text{OH})_2$) by injection of CO_2 in a highly alkaline medium ($2\ \text{m NaOH}$) at ambient temperature ($\sim 20\text{ }^\circ\text{C}$), leading to precipitation of platy-compacted aggregates of dypingite ($\text{Mg}_5(\text{CO}_3)_4(\text{OH})_2\cdot 5\text{H}_2\text{O}$) after 24 h, and (2) complete dypingite-to-magnesite transformation after 24 h by a simple heat-aging step from 20 to $90\text{ }^\circ\text{C}$. The dypingite-to-magnesite transformation implies the simultaneous dehydration and carbonation of a brucitic layer of dypingite coupled with instantaneous formation of magnesite crystals. In this study, the NaOH played a catalytic role; that is, it accelerated brucite carbonation by an increase in carbonate ion concentration with time and it promoted the formation of magnesite during the heat-aging step, as illustrated in the following global reaction: At laboratory scale, magnesite is typically synthesized at high temperature ($>90\text{ }^\circ\text{C}$) and its synthesis requires several days or weeks depending on experimental conditions. For this reason, industrial-scale magnesite production has been limited. The proposed magnesite synthesis method, requiring only 48 h and moderate temperature, could easily be extrapolated on an industrial scale. Moreover, a simple and novel synthesis route for the production of fine platy particles of hydromagnesite is reported, with synthesis requiring only 5 h. On the basis of their chemical compositions and textural properties, there are potential applications for both minerals, for example, as a mineral filler and/or as a flame retardant.



1. INTRODUCTION

The formation and textural properties of natural mineral Mg-carbonates have already been investigated in the past. However, various questions still remain unanswered concerning their formation in natural systems as well as their production at laboratory and industrial scales. Over the past two decades, the precipitation of Mg-carbonates from Mg-rich solutions or Mg-rich suspensions has been actively investigated with a view to the permanent storage of the captured anthropogenic CO_2 via ex situ mineral carbonation, that is, $\text{CO}_2(\text{gas})$ -to-carbonate(solid) transformation (e.g., refs 1–4). Such a carbonation reaction could, therefore, potentially be part of a carbon dioxide capture and storage (CCS) system, which attempts to capture CO_2 from industrial sources and store it permanently. The most successful implementation of this mineral carbonation process involves the extraction of magnesium from natural olivine or serpentines and/or Mg-rich solid waste in aqueous solutions and subsequent precipitation of Mg-carbonate under a CO_2 atmosphere.^{5–10} In addition, the reaction path for the $\text{MgO-H}_2\text{O-CO}_2$ system at ambient temperatures and at atmospheric CO_2 partial pressure is of both geological interest and practical significance. For

example, if the reaction path in this system is known, this would lead to a better understanding of the low-temperature alteration or weathering of mafic and ultramafic rocks. Moreover, exact knowledge of the reaction path in this system is important in order to assess the performance of geological repositories for nuclear waste where mineral periclase (MgO) and brucite ($\text{Mg}(\text{OH})_2$) have been proposed as engineered barriers (e.g., ref 11).

Generally, in the $\text{MgO-H}_2\text{O-CO}_2$ or $\text{Mg}(\text{OH})_2\text{-H}_2\text{O-CO}_2$ slurry systems, a significant number of hydrated and basic (or hydroxylated) carbonates (e.g., nesquehontite, lansfordite, artinite, hydromagnesite, dypingite, pokrovskite, etc.) can be formed at ambient temperature and at moderate CO_2 pressure ($<55\ \text{bar}$) (refs 1, 12–20, this study). All of these minerals are considered to be metastable compounds with respect to magnesite (anhydrous form: MgCO_3), which is the most stable form of Mg-carbonate. However, the low-temperature

Received: May 14, 2012

Revised: September 25, 2012

Published: September 26, 2012

Table 1. Summary of Experimental Conditions for the Synthesis of Anhydrous and Hydroxylated Mg–Carbonates

exptl label	system	use of NaOH	T_i (°C) ^c	P_i (bar) ^c	heat-aging step	t_r ^c	isobaric/anisobaric	mineral
S0	Mg(OH) ₂ ·H ₂ O-CO ₂	yes	ambient (~26 ^a)	50	not	24 h	anisobaric	dypingite
S1	Mg(OH) ₂ ·H ₂ O-CO ₂	yes	ambient (~26 ^a)	50	from 20 to 90 °C	48 h	anisobaric	magnesite
S2	Mg(OH) ₂ ·H ₂ O-CO ₂	not	ambient (~20)	50	from 20 to 90 °C	48 h	anisobaric	H–M–B composite
S3	Mg(OH) ₂ ·H ₂ O-CO ₂	not	90	50	not	12 days	isobaric ^b	hydromagnesite
S4	Mg(OH) ₂ ·H ₂ O-CO ₂	yes	ambient (~26 ^a)	50	from 26 to 45 °C	10 days	anisobaric	H–E composite
S5	Mg(OH) ₂ ·H ₂ O-CO ₂	yes	ambient (~26 ^a)	50	from 38 to 90 °C	5 h	anisobaric	hydromagnesite

^aTemperature of suspension (including exothermic dissolution of NaOH in water). ^bSynthesis at constant gas (CO₂ + Ar) pressure (90 bar). The consumption of CO₂ was regulated by automatic argon injection. H, hydromagnesite; M, magnesite; B, brucite; E, eitelite. ^c T_i : temperature at which the CO₂ gas was injected. P_i : initial CO₂ pressure in the system. t_r : total reaction time (including heat-aging step).

precipitation of magnesite is kinetically inhibited by the preferential precipitation of some of the hydrated and/or hydroxylated Mg–carbonates mentioned above, possibly due to the high hydration nature of Mg²⁺ ions in solution.²¹ For this reason, the formation of magnesite at ambient temperature is virtually impossible.¹ The minimum reported temperature for magnesite production is about 60–100 °C, and its formation also requires a high CO₂ pressure.^{21–23} In various cases, the magnesite is obtained by transformation of pre-existing hydroxylated Mg–carbonate, such as hydromagnesite.^{18,24} This transition can be very slow; for example, below 150 °C and at moderate pressures, its duration is often in the order of days. Higher temperatures, high salinity, high CO₂ pressure, low magnesium concentration (in a closed system), and the use of organic additives (e.g., monoethylene glycol) are known to accelerate the hydromagnesite-to-magnesite transformation.^{18,25} Reported transformation times are between 2 h at 200 °C in a solution saturated with NaCl, and over 100 days at 110 °C at lower salinity in a closed system. Magnesite formation without any apparent hydromagnesite initially or at an intermediate stage has also been reported under high CO₂ pressures (100–150 bar) and at high temperatures (150–180 °C), for experiments combining the dissolution of Mg–silicates with carbonate precipitation.^{23,26–28} The requirement for high temperatures and high CO₂ pressures to precipitate the magnesite has limited its production at an industrial scale. Moreover, magnesite used as a filler and pigment in paper, paint, rubber, and plastics can sometimes be replaced by synthetic calcite that can be produced in a wide range of lower temperatures and CO₂ pressures.^{29–31} Identifying novel and/or innovative synthesis methods for magnesite at low temperature and low CO₂ pressure still remains a major scientific challenge to obtain a better understanding of its formation in natural systems and to facilitate its production on an industrial scale.

In this context, this study proposes a novel and simple synthesis route for the production of rhombohedral single crystals (<2 μm) of magnesite. This synthesis can be summarized by two main sequential reactions: (1) aqueous carbonation of synthetic brucite (Mg(OH)₂) by injection of CO₂ (50 bar) in a highly alkaline medium (2 *m* of NaOH) at ambient temperature (~20 °C), leading to the precipitation of platy-compacted aggregates of dypingite (Mg₅(CO₃)₄(OH)₂·5H₂O) after 24 h, and (2) complete dypingite-to-magnesite transformation after 24 h by a simple heat-aging step from 20 to 90 °C. The NaOH plays a catalytic role; that is, it accelerates brucite carbonation by increasing the concentration of carbonate ions and promoting the exclusive formation of magnesite during the heat-aging step. Conversely, when the experiment was carried out in the absence of NaOH, incomplete carbonation of brucite was observed and the hydromagnesite became the dominant

Mg–carbonate after the heat-aging step. Here, the solid product contained only about 5% magnesite and is called the hydromagnesite–magnesite–brucite composite hereafter. The specific P_{CO_2} – T conditions required to precipitate pure hydromagnesite as well as hydromagnesite–eitelite and hydromagnesite–magnesite–brucite composites from the Mg(OH)₂·H₂O-CO₂ slurry in the presence/absence of NaOH are also reported. Various analytical tools, such as X-ray diffraction (XRD), field emission gun scanning electron microscopy (FESEM), thermogravimetric analyses (TGA), and N₂ adsorption isotherms, were used to characterize the solid products.

2. MATERIALS AND METHODS

The main experimental conditions required to synthesize magnesite, hydromagnesite, and Mg–carbonate composites are summarized in Table 1, and the experimental procedures are described in detail in the following sections.

2.1. Synthesis of Magnesite (MgCO₃). One liter of high-purity water with an electrical resistivity of 18.2 MΩ·cm, 2 mol of NaOH, and 1 mol of synthetic brucite (Mg(OH)₂, with chemical purity > 95%) were placed in a titanium reactor (autoclave with an internal volume of 2 L). This reactive suspension was immediately stirred during the reaction by means of a constant mechanical stirring system (400 rpm). The temperature of the suspension increased instantaneously to 26 °C due to the exothermic dissolution of NaOH in the system. At this reference temperature, CO₂ (≈2 mol) was immediately injected in the system at a pressure of 50 bar. The carbonation reaction started instantaneously, as attested by the continuous consumption of CO₂ (monitored by a pressure drop in the system) and an increase in temperature during the exothermic carbonation reaction (the maximum temperature reached was ≈38 °C after 1 h of reaction ($\Delta T \approx 12$ °C)). After 24 h of carbonation reaction at ambient (or room) temperature (16–20 °C) (including the exothermic period), a heat-aging step was performed from ambient temperature to 90 °C for a further 24 h. On the basis of preliminary experiments, it was found that the NaOH played a catalytic role; that is, it accelerated brucite carbonation by an increase in carbonate ion concentration with time and promoted the formation of magnesite during the heat-aging step. More details are provided in the Results and Discussion section.

At the end of the experiment, the autoclave was removed from the heating system and immersed in cold water. The residual CO₂ was degassed from the reactor during the water-cooling period. After water-cooling at 30 °C (for about 15 min), the autoclave was disassembled, and the solid product was carefully recovered and separated by centrifugation (30 min at 12 000 rpm), decanting the supernatant solutions. The solid product was washed twice by redispersion/centrifugation processes in order to remove the soluble sodium carbonates formed during the synthesis. Finally, the solid product was dried directly in the centrifugation flasks at 80 °C for 48 h. The dry solid product was manually recovered and stored in plastic flasks for subsequent characterization (FESEM, XRD, TGA, and N₂ sorption isotherms).

2.2. Synthesis of Hydromagnesite ($\text{Mg}_5(\text{CO}_3)_4(\text{OH})_2 \cdot 4\text{H}_2\text{O}$).

Two methods are reported in this study:

- Precipitation of hydromagnesite from a $\text{Mg}(\text{OH})_2\text{-H}_2\text{O-CO}_2$ slurry. One liter of high-purity water with an electrical resistivity of $18.2 \text{ M}\Omega\text{-cm}$ and 1 mol of synthetic brucite ($\text{Mg}(\text{OH})_2$) with a chemical purity > 95% were placed in a titanium reactor (autoclave with an internal volume of 2 L). This reactive suspension was immediately stirred at 400 rpm and heated to 90°C . Once the temperature had stabilized, CO_2 was injected at a pressure of 50 bar and the total pressure in the system was immediately increased from 50 to 90 bar by argon injection. At these T and P conditions, the vapor phase primarily consists of a mixture of $\text{Ar} + \text{CO}_2$, with CO_2 in a supercritical state. The reaction time in this solid–liquid–gas thiphasic experiment ($\text{Mg}(\text{OH})_2\text{-H}_2\text{O-CO}_2$ slurry) was typically 12 days in order to obtain high-purity hydromagnesite. The solid product recovery/drying procedures were similar to those described above for the synthesis of magnesite.
- Knowing the catalytic action of NaOH on brucite carbonation, a faster method was implemented to synthesize hydromagnesite. This simple method required only 5 h of carbonation reaction. In fact, this method is very similar to the synthesis method for magnesite (see above) except for the reaction time in each carbonation step: only 3 h for carbonation at ambient temperature (including the exothermic period) and 2 h for the heat-aging step at 90°C were required to obtain high-purity hydromagnesite. The solid product recovery/drying procedures were the same as those described above for magnesite synthesis.

2.3. Synthesis of Mg–Carbonate Composites. Hydromagnesite–Magnesite–Brucite Composite. This composite material was synthesized by making a simple modification to the synthesis method for magnesite (see above). More specifically, the carbonation reaction of brucite was carried out in the absence of NaOH , leading to the formation of hydromagnesite (dominant phase) and magnesite (minor phase). These Mg carbonates were intimately dispersed with residual (or unreacted) brucite, forming a so-called hydromagnesite–magnesite–brucite composite. The solid product recovery/drying procedures were similar to those described above for the synthesis of magnesite, although, in this case, the solid product washing procedure to remove soluble Na carbonate was not necessary for this synthesis.

Hydromagnesite–Eitelite Composite. This composite material was synthesized by making simple modifications to the synthesis method for magnesite (see above). In this case, a heat-aging step at 45°C was performed immediately after CO_2 injection into the system. The reaction time in this $\text{Mg}(\text{OH})_2\text{-H}_2\text{O-NaOH-CO}_2$ system was typically 10 days in order to obtain a hydromagnesite–eitelite binary composite. In this particular case, it was found that the sodium initially contained in NaOH reacted significantly to produce the eitelite mineral ($\text{Na}_2\text{CO}_3\cdot\text{MgCO}_3$). Therefore, in this case, the NaOH had not just a catalytic affect because sodium was also incorporated in the mineral phase. The solid product recovery/drying procedures were the same as those described above for magnesite synthesis.

2.4. Characterization of Solid Products. FESEM Observations. Magnesite, hydromagnesite, and various Mg–carbonate composites were dispersed by ultrasonic treatment in absolute ethanol for 5–10 min. One or two droplets of the suspension were then deposited directly on an aluminum support for SEM observations and coated with platinum. The morphology of various selected powders was observed using a Zeiss Ultra 55 field emission gun scanning electron microscope (FESEM) with a maximum spatial resolution of approximately 1 nm at 15 kV.

XRD Measurements. X-ray powder diffraction (XRD) analyses were performed using a Siemens D5000 diffractometer in Bragg–Brentano geometry; equipped with a θ – θ goniometer with a rotating sample holder. The XRD patterns were collected using $\text{Cu } \alpha_1$ ($\lambda_{\text{Cu}\alpha_1} = 1.5406 \text{ \AA}$) and α_2 ($\lambda_{\text{Cu}\alpha_2} = 1.5444 \text{ \AA}$) radiation in the range of $2\theta = 10\text{--}70^\circ$ with a step size of 0.04° and a counting time of 6 s per step.

Thermogravimetric Analyses. TGA analyses for all Mg–carbonate samples were performed with a Mettler Toledo TGA/SDTA 851e

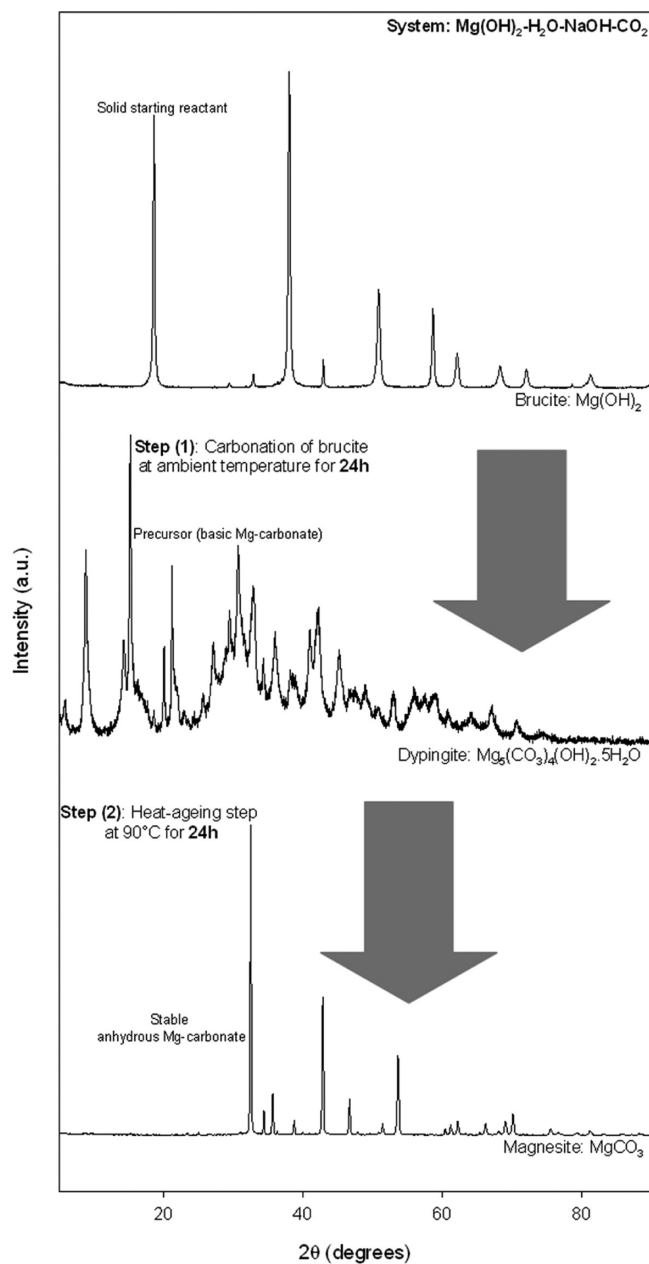


Figure 1. Fast precipitation of magnesite from a $\text{Mg}(\text{OH})_2\text{-H}_2\text{O-CO}_2$ slurry, enhanced by NaOH and a heat-aging step from ambient temperature to 90°C . Only 48 h was required to produce high-purity magnesite as attested from the XRD pattern (ICDD no. 086-2346). Precursor or basic Mg–carbonate was identified as dypingite from the XRD pattern (ICDD no. 023-1218). High-purity synthetic brucite was used as a solid starting reactant, as attested from the XRD pattern (ICDD no. 083-0114).

instrument under the following conditions: a sample mass of about 10 mg, $150 \mu\text{L}$ alumina crucible with a pinhole, heating rate of 5°C min^{-1} , and an inert N_2 atmosphere of 50 mL min^{-1} . The sample mass loss and associated thermal effects were obtained by TGA/SDTA. To identify the different mass loss steps, the TGA first derivative (rate of mass loss) was used. The TGA apparatus was calibrated in terms of mass and temperature. Calcium oxalate was used for the sample mass calibration. The melting points of three compounds (indium, aluminum, and copper) obtained from the DTA signals were used for the sample temperature calibration.

N_2 Sorption Isotherms. N_2 sorption isotherms for magnesite, hydromagnesite, and Mg–carbonate composites were obtained by

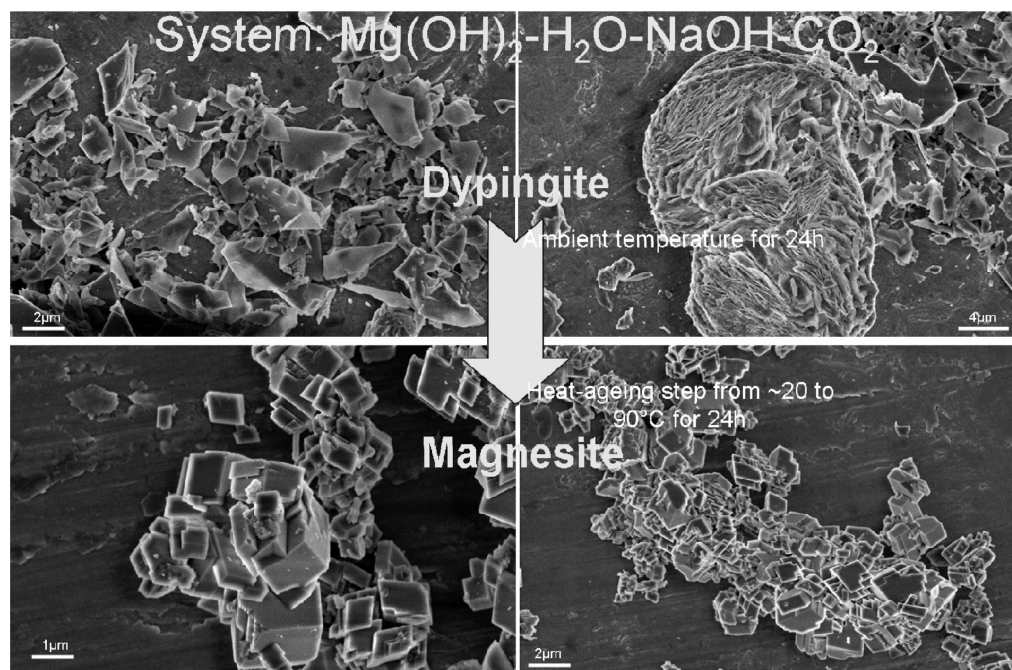


Figure 2. FESEM images showing the morphology of the dypingite precursor and magnesite crystals precipitated from the $\text{Mg}(\text{OH})_2\text{-H}_2\text{O-NaOH-CO}_2$ system at ambient temperature and after a heat-aging step at 90°C , respectively.

Table 2. Mineral Composition, Morphology, and Specific Surface Area (S_{BET}) for Synthesized Mg–Carbonates Deduced from XRD, TGA, FESEM, and N_2 Adsorption Isotherms

expt. label	main mineral(s)	formula	minor mineral(s) (<5%)	morphology	S_{BET} (m^2/g)
S0	dypingite	$\text{Mg}_5(\text{CO}_3)_4(\text{OH})_2 \cdot 5\text{H}_2\text{O}$	eitelite	platy-compacted aggregates	9
S1	magnesite	MgCO_3	eitelite + hydromagnesite	rhombohedral crystals	3
S2	hydromagnesite	$\text{Mg}_5(\text{CO}_3)_4(\text{OH})_2 \cdot 4\text{H}_2\text{O}$	not detected	platy-compacted aggregates	6
	magnesite	MgCO_3		rhombohedral crystals	
	brucite	$\text{Mg}(\text{OH})_2$		hexagonal crystals	
S3	hydromagnesite	$\text{Mg}_5(\text{CO}_3)_4(\text{OH})_2 \cdot 4\text{H}_2\text{O}$	brucite	platy fine particles	23
S4	hydromagnesite	$\text{Mg}_5(\text{CO}_3)_4(\text{OH})_2 \cdot 4\text{H}_2\text{O}$	brucite	irregular aggregation	11
	eitelite	$\text{Na}_2\text{CO}_3 \cdot \text{MgCO}_3$			
S5	hydromagnesite	$\text{Mg}_5(\text{CO}_3)_4(\text{OH})_2 \cdot 4\text{H}_2\text{O}$	brucite	platy fine particles	28

using a sorptomatic system (Thermo Electron Corporation). The specific surface area of powdered samples was estimated by applying the Brunauer–Emmett–Teller (BET) equation in the $0.05 \leq P/P_0 \leq 0.35$ interval of relative pressure and based on a value of 16.2 \AA^2 for the cross-sectional area of molecular N_2 . A nonlinear regression by the least-squares method was performed to fit the interval data (n_{ads} vs P/P_0) in the experimental isotherms.

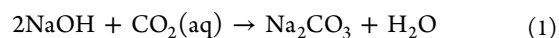
3. RESULTS AND DISCUSSION

3.1. Magnesite Precipitation: Physicochemical Steps and Reaction Mechanism. The precipitation of magnesite at low temperature is kinetically inhibited by the preferential precipitation of hydrated and/or hydroxylated Mg–carbonates (e.g., nesquehontite, lansfordite, artinite, hydromagnesite, dypingite, pokrovskite, etc.), possibly due to the high hydration nature of Mg^{2+} ions in solution.²¹ On the basis of this assumption, the formation of magnesite at ambient temperature is virtually impossible.¹

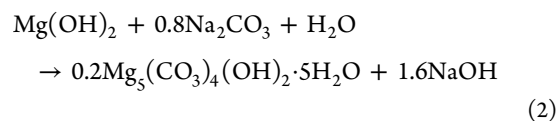
A simple and novel synthesis route for the formation of rhombohedral single crystals ($<2 \mu\text{m}$) of magnesite is described here. The precipitation process requires only 48 h and can be summarized by two main sequential steps (see Figure 1):

- (1) Aqueous carbonation of synthetic brucite ($\text{Mg}(\text{OH})_2$) by injection of CO_2 in a highly alkaline medium (2 m NaOH) at ambient temperature ($\sim 20^\circ\text{C}$). This physicochemical step led to the precipitation of platy-compacted aggregates of dypingite ($\text{Mg}_5(\text{CO}_3)_4(\text{OH})_2 \cdot 5\text{H}_2\text{O}$) after 24 h of fluid–solid interaction, as attested by XRD and FESEM observations on the solid (see Figures 1 and 2). Moreover, a moderate specific surface area ($9 \text{ m}^2/\text{g}$) was deduced from the N_2 adsorption isotherm (Table 2).

Assuming that CO_2 absorption in the highly alkaline solution of NaOH is faster and greater than in water via the following exothermic reaction



the carbonation of brucite leading to the precipitation of dypingite can be written as follows:



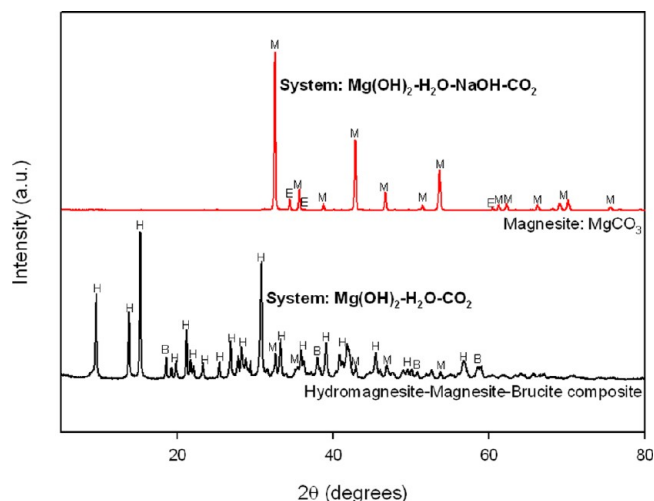
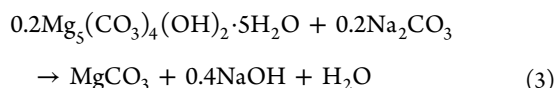


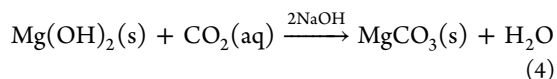
Figure 3. XRD patterns showing the aqueous carbonation of brucite $\text{Mg}(\text{OH})_2$ in the presence and absence of NaOH. The sodium hydroxide played a catalytic role to precipitate the magnesite after only 48 h of reaction. Experimental XRD patterns matching magnesite (M: ICDD no. 086-2346), hydromagnesite (H: ICDD no. 070-0361), eitelite (E: ICDD no. 024-1227), and brucite (B: ICDD no. 044-1482).

These two coupled reactions take place at ambient temperature ($\sim 20^\circ\text{C}$) for the first 24 h. However, as observed in the experiments, these reactions are exothermic, with the suspension temperature reaching a maximum value of $38 \pm 1^\circ\text{C}$ after about 1 h of reaction. The maximum value of the temperature remains constant for about 2 h, and then it decreases slowly to ambient temperature ($\sim 20^\circ\text{C}$).

- (2) A heat-aging step from 20 to 90°C was performed to obtain complete transformation of dypingite to magnesite after 24 h. This assumes a solid-state transition, implying the simultaneous dehydration and carbonation of a brucitic layer of dypingite precursor coupled with instantaneous formation of magnesite crystals. However, the dissolution of the dypingite precursor coupled with magnesite precipitation cannot be excluded. The general reaction for the dypingite-to-magnesite transformation can be written as follows:



In this study, NaOH played a catalytic role; that is, it accelerated brucite carbonation by an increase in carbonate ion concentration with time. The catalytic role can be verified by adding reactions 1–3. The presence of NaOH also promoted magnesite formation during the heat-aging step. In this way, the precipitation of magnesite, enhanced by NaOH and a heat-aging step, can be illustrated by the following global carbonation reaction:



This reaction takes place exclusively when NaOH is used as a catalytic agent. Conversely, if the same

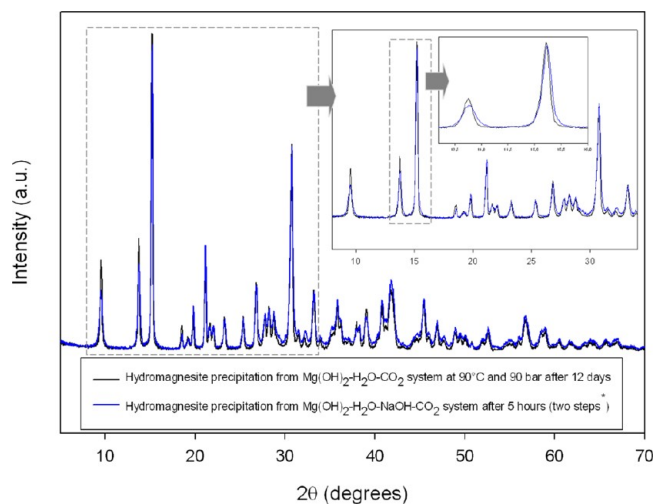
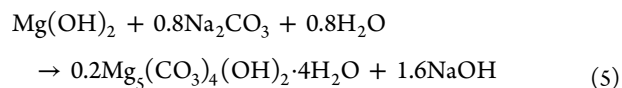


Figure 4. Experimental XRD patterns corresponding to hydromagnesite (ICDD no. 070-0361) synthesized from the $\text{Mg}(\text{OH})_2\text{-H}_2\text{O-CO}_2$ system in the absence and presence of NaOH, and S2 and S5 syntheses in Tables 1 and 2, respectively. (*): (1) carbonation of brucite without external heating for 3 h, followed by (2) heat-aging step from 38 to 90°C for 2 h.

experiment is carried out in the absence of NaOH, incomplete carbonation of brucite is observed and hydromagnesite is the dominant Mg–carbonate after the heat-aging step. In such a case, the hydromagnesite–magnesite–brucite composite obtained contains only about 5% magnesite (see Figure 3).

3.2. Synthesis of Hydromagnesite. Hydromagnesite ($\text{Mg}_5(\text{CO}_3)_4(\text{OH})_2 \cdot 4\text{H}_2\text{O}$) is a naturally occurring compound found in magnesium-rich minerals, such as serpentine, and altered magnesium-rich igneous rocks. It is also produced by alteration of brucite in periclase marbles. In view of its potential use in industrial applications, several scientific studies, technical reports, and patents have been published concerning its synthesis at the laboratory scale (e.g., ref 19).

Two different methods for synthesizing hydromagnesite under laboratory conditions are reported here; both methods can be used to synthesize high-purity hydromagnesite, as attested by X-ray diffraction observations on the powder products where the experimental XRD patterns successfully match with the ICDD card no. 070-0361 (see Figure 4). Platy fine particles with a moderate specific surface area ($>20\text{m}^2/\text{g}$) were obtained for both methods (see Table 2 and FESEM image for synthesis of S3 in Figure 5). However, the synthesis time is drastically reduced from 12 days to 5 h when NaOH is used as a catalyst and/or additive in the $\text{Mg}(\text{OH})_2\text{-H}_2\text{O-CO}_2$ system. Similar to the synthesis of magnesite, the NaOH-rich solution accelerates brucite carbonation by an increase in carbonate ion concentration with time. For this case, the general reaction for hydromagnesite precipitation, that is, an intermediate hydroxylated (or basic) Mg–carbonate with respect to magnesite, can be written as follows:



As mentioned above, this carbonation reaction of brucite takes only 5 h. Conversely, the hydrothermal carbonation of brucite in the absence of NaOH takes about 12 days to obtain

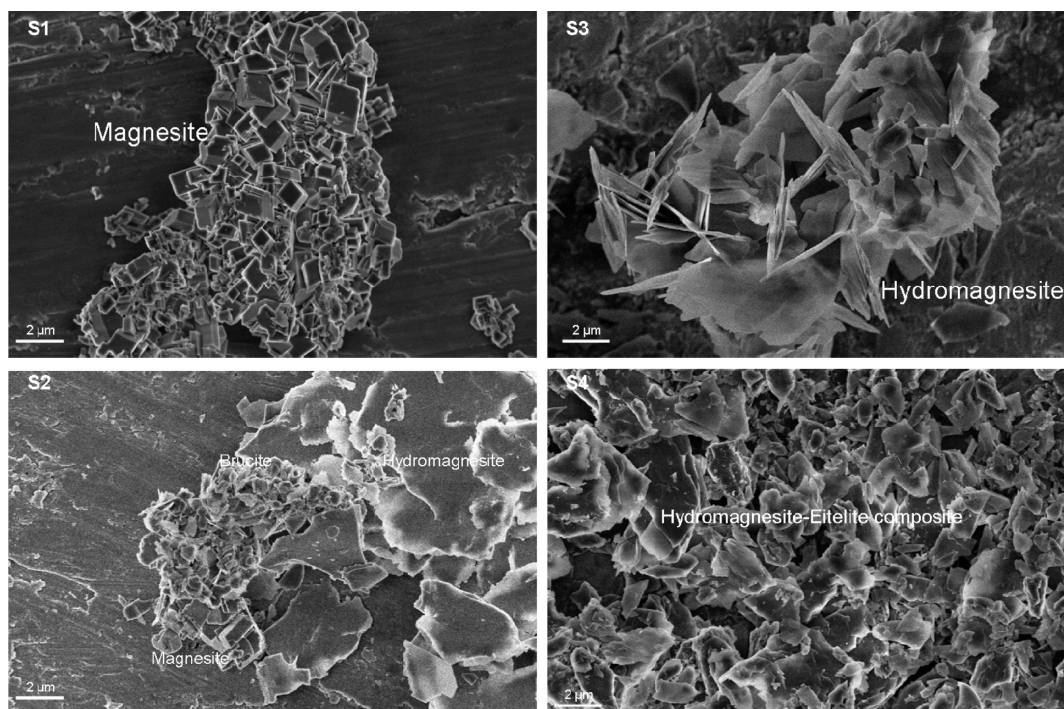
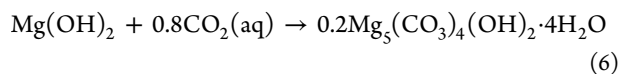


Figure 5. FESEM images showing the morphology of magnesite (S1), hydromagnesite (S3), hydromagnesite–magnesite–brucite composite (S2), and hydromagnesite–eitelite composite (S4) precipitated from the $\text{Mg}(\text{OH})_2\text{-H}_2\text{O-CO}_2$ system in the presence/absence of NaOH. Specific experimental conditions for these syntheses are reported in Table 1.

hydromagnesite with similar textural properties. The hydrothermal carbonation of brucite to form hydromagnesite at 90 °C and 90 bar and in the absence of NaOH can be described by the following global reaction.

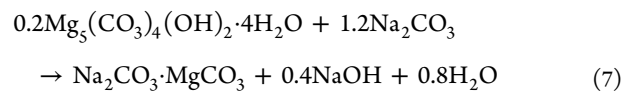


In conclusion, the use of NaOH as a catalyst is a powerful option to accelerate the production of hydromagnesite (only 5 h) with potential industrial applications given its advantageous textural properties and composition, as reported in Table 2.

3.3. Synthesis of Mg–Carbonate Composites. As mentioned in the Introduction, magnesite is considered to be the most stable Mg–carbonate compound. However, its precipitation at low temperature is kinetically inhibited by the preferential precipitation of hydrated and/or hydroxylated Mg–carbonates, possibly due to the high hydration nature of Mg^{2+} ions in solution.²¹ On the basis of these concepts, the formation of anhydrous Mg–carbonates (e.g., magnesite and dolomite) at ambient temperature is virtually impossible.¹ However, anhydrous eitelite ($\text{Na}_2\text{CO}_3 \cdot \text{MgCO}_3$) can be formed at low temperature.³² This mineral is not found in large quantities in natural sedimentary environments, but its anhydrous form is certainly of interest for understanding how Mg in solution can be dehydrated to form anhydrous Mg carbonates at low temperature.

In the present study, the catalytic role of NaOH has been demonstrated for rapid precipitation of magnesite (reactions 1–4) and hydromagnesite (reaction 5) (see also Tables 1 and 2). However, under specific conditions (see S4 in Table 1), the sodium dissolved during the carbonation process may react significantly after 10 days to form an atypical hydromagnesite–eitelite composite at low temperature (45 °C). Both minerals were clearly identified by X-ray diffraction on the solid product,

and the experimental XRD pattern obtained successfully matched the ICDD card no. 070-0361 for hydromagnesite and no. 024-1227 for eitelite (see S4 in Figure 6). FESEM observations have revealed irregular fine aggregates (S4 in Figure 5), and a moderate specific surface area (11 m^2/g) was deduced from the N_2 adsorption isotherm (see also Table 2). It is assumed that hydromagnesite is initially formed in this system, according to reaction 5, followed by the precipitation of eitelite. In such a case, two explanations are possible: (i) dissolution of hydromagnesite (so-called precursor) coupled with eitelite precipitation or (ii) a solid-state transition, implying the simultaneous dehydration and carbonation of a brucitic layer of hydromagnesite precursor coupled with the progressive formation of eitelite crystals. The general reaction for hydromagnesite-to-eitelite transformation can be written as follows:



This reaction cannot be completed because only 1 mol of Na_2CO_3 can be produced in the system; see reaction 1. For this reason, the solid recovered after 10 days of reaction contains mainly hydromagnesite and eitelite minerals, the so-called hydromagnesite–eitelite composite in the present study.

On the other hand, as mentioned in section 3.1, the carbonation of brucite in the absence of NaOH leads to incomplete brucite carbonation after a heat-aging step (S2 synthesis) where the mineral composition of the recovered solid was hydromagnesite, magnesite, and residual brucite (see Figures 3 and 6). More specific information on the experimental conditions, composition, and textural properties are provided in Tables 1 and 2. For this case, the hydromagnesite formation is in agreement with reaction 6, where a small proportion of hydromagnesite was transformed into magnesite by the following classical reaction:

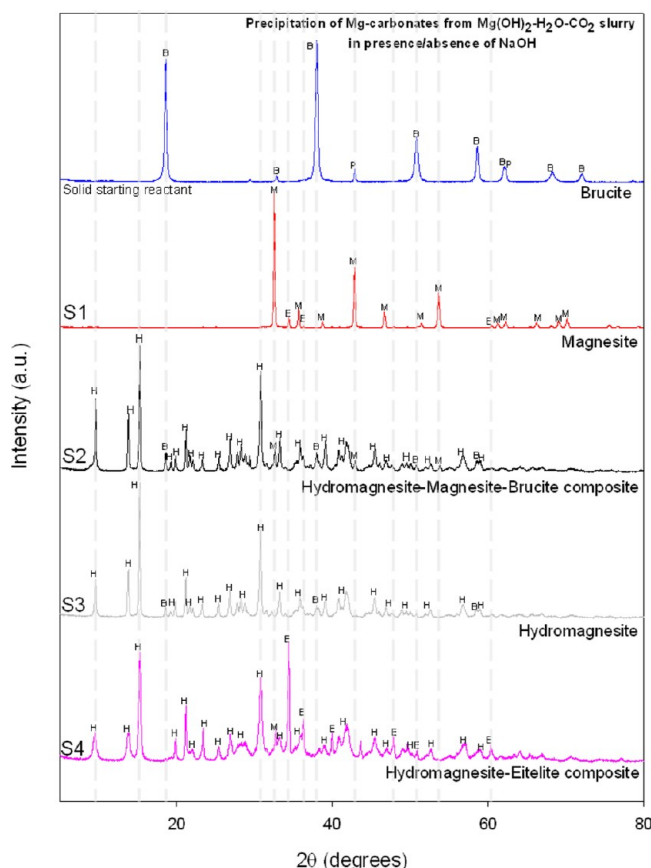
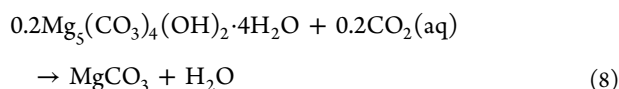


Figure 6. Characterization by X-ray diffraction of the solid starting reactant (brucite) and the solid products recovered after brucite carbonation in the presence or absence of NaOH (syntheses: S1, S2, S3, and S4). Experimental XRD patterns matching magnesite (M: ICDD no. 086-2346), hydromagnesite (H: ICDD no. 070-0361), eitelite (E: ICDD no. 024-1227), and brucite (B: ICDD no. 044-1482).



In general, higher temperatures (>150 °C), high salinity, high CO₂ pressure, low magnesium concentration (in a closed system), and the use of organic additives (e.g., monoethylene glycol) are known to accelerate the hydromagnesite-to-magnesite transformation.^{18,25}

3.4. Potential Industrial Applications. In general, anhydrous Mg-carbonates (e.g., magnesite, eitelite, dolomite, etc.) and intermediate basic magnesium carbonates (e.g., dypingite, hydromagnesite, artinite, pokrovskite, etc.) with a controlled morphology and particle size and a moderate-to-high specific surface area have great potential for use in applications, such as a mineral filler and pigment in paper, paint, rubber, and plastics, and could also be used as flame retardants. Unfortunately, the production at an industrial scale has been limited because high pressures, high temperatures, and long production times are frequently required. The present study shows how high-purity magnesite can be produced after 48 h of reaction and how high-purity hydromagnesite can be produced after 5 h of reaction. On the basis of its composition and textural properties, the magnesite could be used as a mineral filler in paper and pigments. Moreover, additional applications, such as a flame retardant in electrical and electronic parts, construction

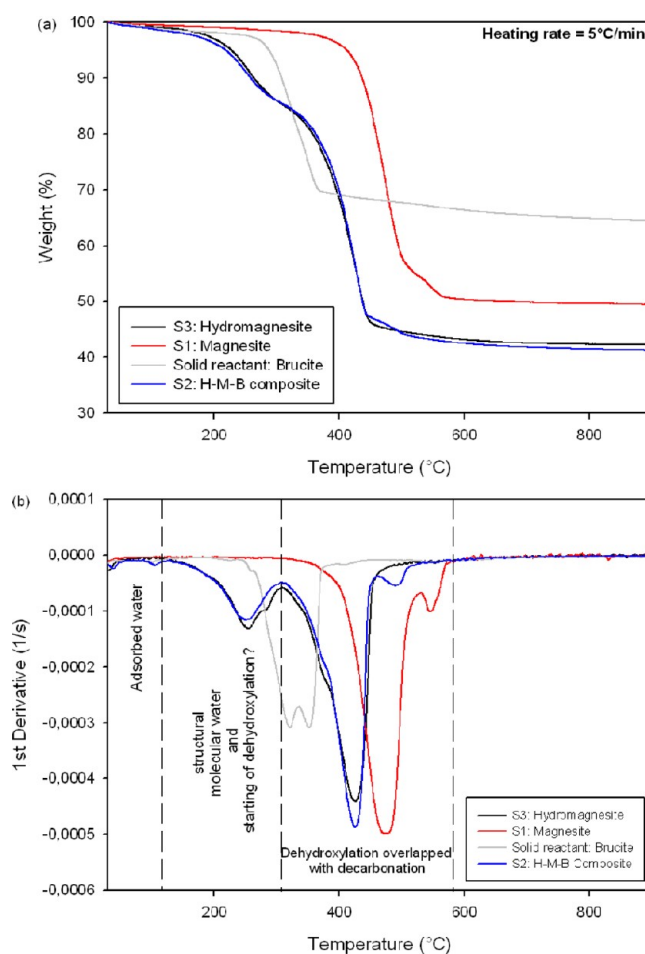


Figure 7. Thermogravimetric analyses (TGA on top graph and differential TGA on bottom graph) of synthesized magnesite (S1), hydromagnesite (S3), and hydromagnesite–magnesite–brucite composite (S2).

materials, etc., can be envisaged for hydromagnesite because their dehydration–dehydroxylation–decarbonation processes consume a significant amount of energy in a broad interval of temperature (see Figure 7). Moreover, the platy fine particles and moderate specific surface area (28 m²/g) of hydromagnesite can facilitate its dispersion/distribution when used as a mineral filler or flame retardant.

4. CONCLUSION

This study proposes a simple and novel synthesis route for the production of rhombohedral single crystals (<2 μm) of magnesite and platy fine particles of hydromagnesite. It also demonstrates the catalytic action of NaOH during the carbonation process of brucite mineral, leading to fast precipitation of high-purity magnesite after 48 h of reaction and fast precipitation of high-purity hydromagnesite after only 5 h of reaction. For each case, a global reaction mechanism has been proposed. Finally, it is worth noting that both minerals could have good potential for use as a mineral filler and/or as a flame retardant.

AUTHOR INFORMATION

Corresponding Author

*E-mail: german.montes-hernandez@ujf-grenoble.fr.

Notes

The authors declare no competing financial interest.

ACKNOWLEDGMENTS

The authors are grateful to the French National Center for Scientific Research (CNRS) and the University Joseph Fourier in Grenoble for providing financial support.

REFERENCES

- (1) Hanchen, M.; Prigiobbe, V.; Baciocchi, R.; Mazzotti, M. *Chem. Eng. Sci.* **2008**, *63*, 1012.
- (2) Saldi, G. D.; Jordan, G.; Schott, J.; Oelkers, E. H. *Geochim. Cosmochim. Acta* **2009**, *73*, 5646.
- (3) Zhao, L.; Sang, L.; Chen, J.; Ji, J.; Teng, H. H. *Environ. Sci. Technol.* **2010**, *44*, 406.
- (4) Benezeth, P.; Saldi, G. D.; Dandurand, J.-L.; Schott, J. *Chem. Geol.* **2011**, *286*, 21.
- (5) IPCC (Intergovernmental Panel on Climate Change) *Special Report on Carbon Dioxide Capture and Storage*; Cambridge University Press: Cambridge, U.K., 2005.
- (6) O'Connor, W. K.; Dahlin, C. L.; Rush, G. E.; Gerdemann, S. J.; Penner, L. R.; Nilsen, D. N. *Aqueous Mineral Carbonation: Mineral Availability, Pretreatment, Reaction Parametrics, and Process Studies*; Technical Report DOE/ARC-TR-04-002; U.S. Department of Energy: Washington, DC, 2005.
- (7) Munz, I. A.; Kihle, J.; Brandvoll, O.; Machenbach, I.; Carey, J. W.; Haug, T. A.; Johansen, H.; Eldrup, N. *Energy Procedia* **2009**, *1*, 4891.
- (8) Lin, P.-C.; Huang, C.-W.; Hsiao, C.-T.; Teng, H. *Environ. Sci. Technol.* **2008**, *42*, 2748.
- (9) Sun, Y.; Parikh, V.; Zhang, L. *J. Hazard. Mater.* **2012**, *209–210*, 458.
- (10) Bobicki, E. R.; Liu, Q.; Xu, Z.; Zeng, H. *Prog. Energy Combust. Sci.* **2012**, *38*, 302.
- (11) Xiong, Y.; Lord, A. S. *Appl. Geochem.* **2008**, *23*, 1634.
- (12) Langmuir, D. *J. Geol.* **1965**, *73*, 730.
- (13) Oh, K. D.; Morikawa, H.; Iwai, S.-I.; Aoki, H. *Am. Mineral.* **1973**, *58*, 339.
- (14) Hales, M. C.; Frost, R. L.; Martens, W. J. *Raman Spectrosc.* **2008**, *39*, 1141.
- (15) Deelman, J. C. *Neues Jahrb. Mineral., Monatsh.* **1999**, *7*, 289.
- (16) Deelman, J. C. *Notebooks on Geology* **2003**, Letter 2003/03 (CG2003_L03_JCD).
- (17) Zhang, Z.; Zheng, Y.; Ni, Y.; Liu, Z.; Chen, J.; Liang, X. *J. Phys. Chem. B* **2006**, *110*, 12969.
- (18) Sandengen, K.; Josang, L. O.; Kaasa, B. *Ind. Eng. Chem. Res.* **2008**, *47*, 1002.
- (19) Pohl, M.; Rainer, C.; Esser, M. European Patent Application EP 2 322 581 A1, 2011.
- (20) Fournier, J. Report 2022153401; Research Center: Richmond, VA, 1992.
- (21) Deelman, J. C. *Chem. Erde* **2001**, *61*, 224.
- (22) Usdowski, E. *Naturwissenschaften* **1989**, *76*, 374.
- (23) Giammar, D. E.; Bruant, R. G., Jr.; Peters, C. A. *Chem. Geol.* **2005**, *217*, 257.
- (24) Stevula, L.; Petrovic, J.; Kubranova, M. *Chem. Zvesti* **1978**, *32*, 441.
- (25) Zhang, L. Technical Report SAN099-19465; Sandia National Laboratories: Albuquerque, NM, 2000.
- (26) Bearat, H.; Mckelvy, M. J.; Chizmeshya, A. V. G.; Gormley, D.; Nunez, R.; Carpenter, R. W.; Squires, K.; Wolf, G. H. *Environ. Sci. Technol.* **2006**, *40*, 4802.
- (27) Wolf, G. H.; Chizmeshya, A. V. G.; Diefenbacher, J.; Mckelvy, M. *J. Environ. Sci. Technol.* **2004**, *38*, 932.
- (28) O'Connor, W. K.; Dahlin, D. C.; Rush, G. E.; Dahlin, C. L.; Collins, W. K. *Miner. Metall. Process.* **2002**, *19*, 95.
- (29) Montes-Hernandez, G.; Renard, F.; Geffroy, N.; Charlet, L.; Pironon, J. *J. Cryst. Growth* **2007**, *308*, 228.
- (30) Montes-Hernandez, G.; Fernandez-Martinez, A.; Renard, F. *Cryst. Growth Des.* **2009**, *9*, 4567.
- (31) Montes-Hernandez, G.; Daval, D.; Chiriac, R.; Renard, F. *Cryst. Growth Des.* **2010**, *10*, 4823.
- (32) Deelman, J. C. *Neues Jahrb. Mineral., Monatsh.* **1984**, *H10*, 468.